AN INTEGRATED GRAPH CUTS SEGMENTATION AND PIECE-WISE CONVEX UNMIXING APPROACH FOR HYPERSPECTRAL IMAGING

Pegah Massoudifar, Anand Rangarajan, Alina Zare† *and Paul Gader*

Dept. of Computer and Information Science and Engineering
University of Florida, Gainesville, FL, USA

ABSTRACT

Context-based unmixing has been studied by several researchers. Recent techniques, such as piece-wise convex unmixing using fuzzy and possibilistic clustering or Bayesian methods proposed in [11] attempt to form contexts via clustering. It is assumed that the linear mixing model applies to each cluster (context) and endmembers and abundances are found for each cluster. As the clusters are spatially coherent, hyperspectral image segmentation can significantly aid unmixing approaches that perform cluster specific estimation of endmembers. In this work, we integrate a graph-cuts segmentation algorithm with piece-wise convex unmixing. This is compared to fuzzy clustering (FCM) with results obtained on two datasets. The results demonstrate that the integrated approach achieves better segmentation and more precise endmember identification (in terms of comparisons with known ground truth).

Index Terms— endmember extraction, hyperspectral image analysis, graph cuts, Markov random fields, piece-wise convex, segmentation

1. INTRODUCTION

The past decade has seen an upsurge in the acquisition and processing of hyperspectral imagery. Our ability to integrate the disparate information present in different frequencies in hyperspectral images is now mainly limited by the lack of suitable mathematical and algorithmic machinery. In remotely sensed hyperspectral image segmentation, we often need a good segmentation prior to endmember extraction especially when estimating region specific endmembers. Without segmentation, downstream components like endmember extraction suffer since unmixing lacks crucial information regarding spatial coherence.

Motivated by an information integration perspective, we bring together hyperspectral segmentation, endmember extraction and abundance estimation in a coherent manner with each part harmoniously influencing the entire system. First, hyperspectral image segmentation is set up using a Markov random field (MRF) framework with unary segmentation likelihoods and pairwise smoothness priors on the pixels. Subsequently, we show that graph cuts are a suitable algorithmic framework for obtaining good (albeit suboptimal) segmentations. Next, we use the obtained segmentation to drive unmixing. Piece-wise convex endmember extraction and abundance estimation follow—with both depending heavily on the graph cut-based segmentation. The result is an integrated system for hyperspectral image processing called GRENDEL (Graph-based endmember extraction and labeling).

2. PREVIOUS WORK

Unmixing is the process of decomposing each pixel in the image into a set of constituent spectral signatures or endmembers and a set of fractional abundances. Endmembers are usually identified globally while abundances are estimated for each pixel. Statistical approaches used when the spectral mixtures are highly mixed, try to determine both the endmembers and abundance parameters via estimation theory. Sparse regression approaches are also popular and have recently taken advantage of semi-supervised machine learning by assuming the knowledge of a few pure spectral signatures in advance [6]. Generative approaches try to minimize the volume of the simplex with many assuming pixel purity—the presence of at least one pure pixel endmember. Vertex Component Analysis (VCA) [9] which projects data onto the space orthogonal to the subspace of endmembers and Iterative Constrained Endmembers (ICE) [1] which replaces the volume of the simplex with the sum of squared distances between all the simplex vertices are the standard bearers for this class of approaches. All of these methods assume that the image comes from a single convex region—a simplistic assumption in real-world data.

An approach that goes beyond global endmembers is piece-wise convex multiple-model endmember detection (PCOMMEND) [11], wherein the image is divided into several convex regions with linear unmixing performed per region. Convex regions are represented as clusters but this does not leverage the underlying grid. Newer methods exploit the correlation between spatial and spectral neighbors

†Dept. of Electrical and Computer Engineering, University of Missouri, Columbia, MO, USA

and use support vector machine (SVM) training [3], minimum spanning forests [10] or multinomial logistic regression with active learning [6]. Nonlinear unmixing rounds out the set of approaches but we deem these beyond the scope of this work. Finally, we point out the pioneering effort in [8] which employs graph cuts for hyperspectral segmentation. Our work follows in this lineage but carries it forward to include region-based endmember detection.

The above discussion is highly suggestive of the need for integrating segmentation algorithms into piece-wise convex unmixing—the overall goal of this work.

3. GRENDEL: GRAPH-BASED ENDMEMBER EXTRACTION AND LABELING

Unsupervised image segmentation is a challenging problem, mainly addressed by the computer vision community and adapted by us to the hyperspectral realm. A standard approach employs maximum *a posteriori* (MAP) estimation using a Markov random field (MRF) prior with graph cuts as the optimization algorithm of choice. We now briefly describe the approach, first for pedagogical reasons using binary image segmentation as an example, followed by the more realistic case of a hyperspectral image with many intensity levels in each band.

Exact MAP estimation with an MRF prior can be obtained by solving a minimum cut problem on a well defined graph. This is based on the work in [4]—the first to use graph cuts for finding the exact MAP estimate in binary image segmentation. Assume an image X where each pixel is either black or white ($x_i = 0$ if the pixel is black and $x_i = 1$ otherwise). You observe a corrupted image Y with n pixels $y_1, y_2, \ldots, y_n$ conditionally dependent on their corresponding x_i with the conditional density function $p(Y|X) = \Pi_i f(y_i|x_i)$. Since the original image is binary, image estimation and segmentation coincide. The prior distribution on the pixel labels can be written as an MRF with pairwise interactions

$$p(X) \propto \exp\left\{\frac{1}{2}\sum_{ij}\beta_{ij}\left[x_i x_j + (1-x_i)(1-x_j)\right]\right\} \quad (1)$$

where β_{ij} is zero if i and j are not neighbors in the pixel graph $G(V,E)$ and is a constant otherwise. Given the likelihood $p(Y|X)$ and the MRF prior $p(X)$, the posterior maximization problem becomes

$$\hat{X} = \arg\max_X L(X) = \arg\max_X \sum_i \log\left\{\frac{f(y_i|1)}{f(y_i|0)}\right\} x_i + \frac{1}{2}\sum_{ij}\beta_{ij}\left[x_i x_j + (1-x_i)(1-x_j)\right]. \quad (2)$$

The maximization problem in (2) can be equivalently formulated via a minimum cut on the graph $G(V,E)$ of image pixels augmented with a source and sink. If the log-likelihood ratio $\lambda_i \equiv \log\left\{\frac{f(y_i|1)}{f(y_i|0)}\right\}$ is positive, an edge exists from the source to pixel i, else an edge is created from pixel i to the sink. Neighboring pixels $(i,j) \in E$ are connected with an edge weight β_{ij}. A two set partition of the vertices (a.k.a. a graph cut) has a cost

$$\begin{aligned} E(X) &= \sum_{i=1}^{n}\left[x_i \max(0,-\lambda_i) + (1-x_i)\max(0,\lambda_i)\right] \\ &\quad + \frac{1}{2}\sum_{ij}\beta_{ij}(x_i - x_j)^2 \end{aligned} \quad (3)$$

which is proportional to (2) above. Graph algorithms based on the equivalence of maximum flow to the minimum cut can be used to find the minimizer of (3) in polynomial time.

Although the work in [4] was limited to binary images, the graph cut algorithm has expanded to include multiple labels [2] over the past decade. The graph cut approach can be readily adapted for segmenting hyperspectral images with a large number of bands. Here, we observe an image Y with n pixels $\{\mathbf{y}_1, \mathbf{y}_2, \ldots, \mathbf{y}_n\}$ where $\mathbf{y}_i$ denotes a vector of reflectance values at different wavelengths. The MRF neighborhood is again driven by the pixel graph $G(V,E)$. A binary set $S = \{S_1, S_2, \ldots, S_n\}$ represents the segmentation where $S_i = \{s_{i1}, s_{i2}, \ldots s_{iK}\}$ denotes the one-of-K region membership of a pixel ($s_{ia} \in \{0,1\}, \sum_a s_{ia} = 1$). The graph cuts partition cost is

$$E(S) = -\lambda\sum_{i=1}^{n}\sum_{a=1}^{K}\left[s_{ia}\log f(\mathbf{y}_i|\mathrm{reg}_a)\right] + \sum_{ij}\sum_{a=1}^{K}\beta_{ij}s_{ia}s_{ja}\exp\left\{-\frac{\|\mathbf{y}_i-\mathbf{y}_j\|^2}{\sigma^2}\right\}\frac{1}{\mathrm{dist}(i,j)} \quad (4)$$

where "reg" denotes region, $f(\mathbf{y}_i|\mathrm{reg}_a)$ is the region specific density, and $\mathrm{dist}(i,j)$ is the grid distance between pixels. The graph $G(V,E)$ now has multiple terminals each of which represents a segmentation into a particular region. A segmentation with optimal cost is the one that partitions all terminals into isolated segments. This multi-partition graph cut segmentation is a generalization of (3) with multiple labels replacing the binary ones. While this problem is NP-complete, a set of α-expansion moves can efficiently find a good, albeit approximate solution in polynomial time. For more details please see [2].

Piece-wise Convex Endmember Detection (PCOMMEND) [11] extends the single set linear mixing approach by considering the presence of multiple sets of endmembers. In order to achieve this, PCOMMEND divides the image into a specific number of clusters with a clustering algorithm used for

A MATLAB implementation is available at `http://www.wisdom.weizmann.ac.il/~bagon/matlab.html`.

partitioning the image. Clustering is more suitable for vector space patterns that do not have an underlying grid. Consequently, a good segmentation should considerably alleviate PCOMMEND. The principal argument in this paper is that graph cut segmentation integrates well with PCOMMEND since the latter estimates a set of endmembers for each segmentation region. The result is GRENDEL (Graph-based Endmember Extraction and Labeling)—an integrated suite comprising graph cuts driven hyperspectral image segmentation with the extraction of multiple sets of endmembers, one for each region.

4. RESULTS

Below, GRENDEL is tested using simulated and measured hyperspectral data sets. The first data set is Pavia University which is used to compare GRENDEL to PCOMMEND which already outperforms VCA and ICE, followed by the NEON dataset where ground truth endmembers are not available.

The Pavia hyperspectral data set was collected over an urban area of Pavia, in northern Italy by the ROSIS spectrometer on July 8, 2002 [11]. The image contains 610×341 pixels with 103 bands. The ROSIS sensor collected data over the 430–850nm wavelength range at a 4nm spectral sampling interval. The data was collected over the 430–850-nm wavelength range at a 4nm spectral sampling interval. Data has been atmospherically corrected by the German Remote Sensing Data Center of the German Aerospace Center (DLR) [5]. The image contains both natural and urban regions. We applied GRENDEL with the following parameters: $a = 0.6, b = 0.001, C = 2, M = 3$.

We considered 6 different endmembers detected in the Pavia University image which are: Metal roofing, Cement/Sidewalk, shadow, soil, asphalt and vegetation. Comparison results in Fig. 2(a-e) indicate that we have reduced the endmember estimation error in comparison to PCOMMEND (which in the main outperforms VCA and ICE).

Following Pavia, the results of segmenting the NEON dataset are shown (with no endmember comparisons since we don't have ground truth). The National Ecological Observatory Network (NEON) has conducted a series of airborne flights and supporting ground measurements in two study areas located near Gainesville, Florida since 2010. Major plant communities exist within the region and these diverse targets are populated by sandhill, mixed forests, basin swamp, basin marsh, marsh lake, etc. [7]. We conducted manual preprocessing to remove the very noisy bands. The image used in the experiments has 358×317 pixels with 174 different bands. Segmentation comparisons were conducted against fuzzy clustering and visual inspection reveals improvement. Both of the segmentation results are for 5 different clusters shown in gray scale. Graph cuts yields much smoother results than FCM. The roads and the area around the lake in FCM are noisy and with white dots present. These and other artifacts are not present in graph cuts.

5. DISCUSSION

When we seek to estimate multiple sets of endmembers, the spatial coherence of hyperspectral imagery naturally suggests a strong role for segmentation. Consequently, we integrated graph cut-based segmentation approaches with region specific, piece-wise convex endmember detection resulting in GRENDEL. Initial results when compared against ground-truth endmembers are very encouraging with coherent regions leading to more consistent endmembers. Future work will focus on tighter integration with unified estimation of segmentation regions, endmembers and abundances.

6. REFERENCES

[1] M. Berman, H. Kiiveri, R. Lagerstrom, A. Ernst, R. Dunne, and J.F. Huntington. ICE: A statistical approach to identifying endmembers in hyperspectral images. *IEEE Transactions on Geoscience and Remote Sensing*, 42(10):2085–2095, 2004.

[2] Y. Boykov and G. Funka-Lea. Graph cuts and efficient N-D image segmentation. *International Journal of Computer Vision*, 70(2):109–131, 2006.

[3] M. Fauvel, J.A. Benediktsson, J. Chanussot, and J.R. Sveinsson. Spectral and spatial classification of hyperspectral data using SVMs and morphological profiles. *IEEE Transactions on Geoscience and Remote Sensing*, 46(11):3804–3814, 2008.

[4] D.M. Greig, B.T. Porteous, and A.H. Seheult. Exact *maximum a posteriori* estimation for binary images. *Journal of the Royal Statistical Society, Series B*, 51(2):271–279, 1989.

[5] S. Holzwarth, A. Muller, M. Habermeyer, R. Richter, A. Hausold, S. Thiesmann, and P. Strobl. HySens–DAIS/ROSIS Imaging Spectrometers at DLR. In *Proceedings of the 3rd EARSeL Workshop on Imaging Spectroscopy*, pages 3–14, Herrsching, Germany, 2003.

[6] M.-D. Iordache, J.M. Bioucas-Dias, and A. Plaza. Sparse unmixing of hyperspectral data. *IEEE Transactions on Geoscience and Remote Sensing*, 49(6):2014–2039, 2011.

[7] T. Kampea, K. Krausea, C. Meiera, D. Barnetta, and J. McCorkel. The NEON 2010 airborne pathfinder campaign in Florida. *NEON Technical Memo 002*, pages 5–11, 2010.

[8] J. Li, J.M. Bioucas-Dias, and A. Plaza. Hyperspectral image segmentation using a new Bayesian approach with active learning. *IEEE Transactions on Geoscience and Remote Sensing*, 49(10):3947–3960, 2011.

[9] J.M.P. Nascimento and J.M. Bioucas-Dias. Vertex component analysis: A fast algorithm to unmix hyperspectral data. *IEEE Transactions on Geoscience and Remote Sensing*, 43(4):898–910, 2005.

[10] Y. Tarabalka, J.A. Benediktsson, and J. Chanussot. Spectral-spatial classification of hyperspectral imagery based on partitional clustering techniques. *IEEE Transactions on Geoscience and Remote Sensing*, 47(8):2973–2987, 2009.

[11] A. Zare, P.D. Gader, O. Bchir, and H. Frigui. Piecewise convex multiple-model endmember detection and spectral unmixing. *IEEE Transactions on Geoscience and Remote Sensing*, 51(5-1):2853–2862, 2013.

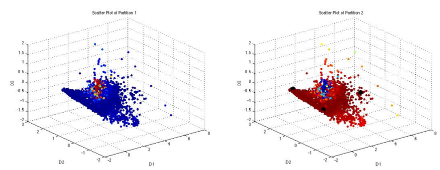

Fig. 1. Scatter plots of partition 1 and 2.

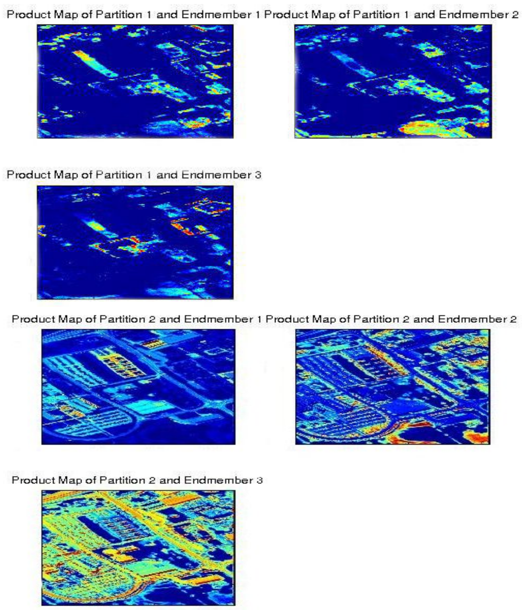

Fig. 2. GRENDEL product maps for HySens Pavia University. Endmembers with high membership for each data point are highlighted. Product maps associated with endmembers 1, 2, and 5 (3, 4 and 6) correspond to partition 1 (2). Partitions 1 and 2 can be interpreted as endmembers corresponding to man-made and natural materials respectively. The color scale ranges from (dark blue) zero to (red) one.

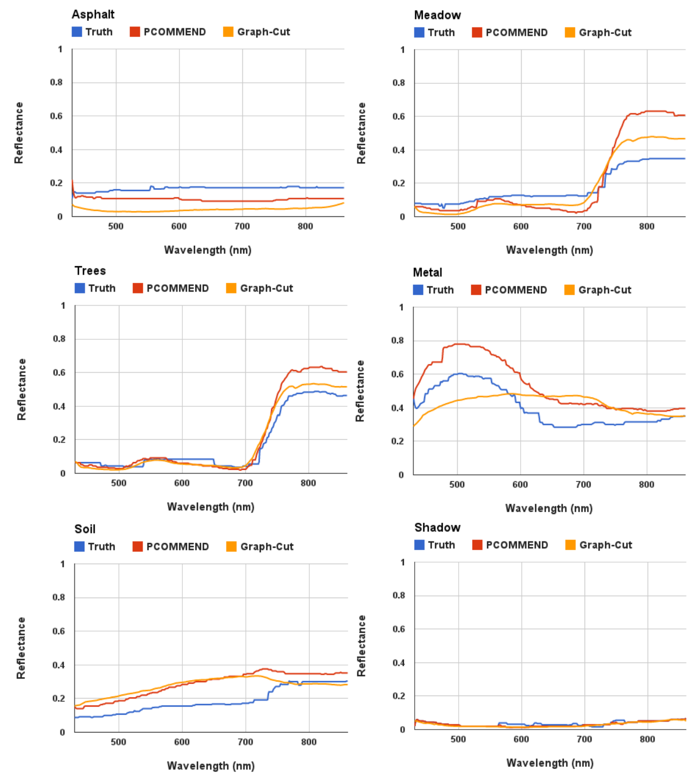

Fig. 3. Comparison between the endmembers found by GRENDEL, PCOMMEND and Pavia ground-truth: GRENDEL endmembers (yellow) and PCOMMEND endmembers (red). The mean spectrum and ±1 standard deviation of the pixels from the ground-truth class in the Pavia University test set are shown in blue. The y-axis is in reflectance units and the x-axis corresponds to wavelength (in nanometers).

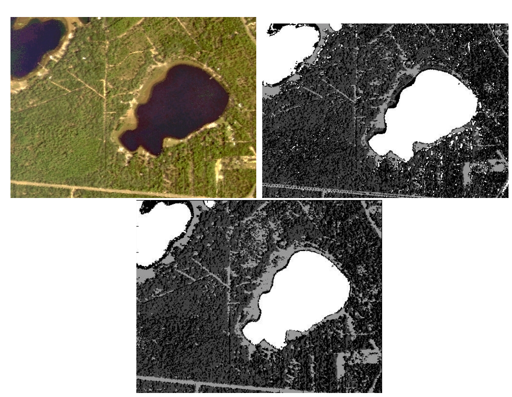

Fig. 4. Top left: NEON image. Top right: fuzzy C-means segmentation. Bottom: graph-cut segmentation